MULTIAXIAL FATIGUE LOW CYCLE FATIGUE TESTING

S.Y. Zamrik
Engineering Science and Mechanics Department
The Pennsylvania State University
University Park, Pennsylvania 16802

Multiaxial testing methods are reviewed. Advantages and disadvantages of each type test is discussed. Significant multiaxial data available in the literature is analyzed. The yield theories are compared for multiaxial fatigue analysis.

INTRODUCTION

Multiaxial Fatigue Analysis is becoming an essential element in estimating the life of structural components. For example, at elevated temperature, most structural components experience a multiaxial stress condition either due to geometrical configuration, or to temperature variation or to both.

Generally, multiaxial fatigue analysis is based on some type of correlation that can be related to uniaxial data. The main reason for such an approach is the lack of sufficient multiaxial fatigue data and to the difficulty in producing such data.

In the early work of Manson-Coffin (1) it was recognized that, in low cycle fatigue, plastic strain and not stress can be well measured and related to life. Based on this observation, the static yield theories became the favorite approach to analyzing multiaxial fatigue. The most widely used criteria are the maximum shear strain (Tresca's) theory and the maximum distortion energy theory (Von-Mises). These two static yield theories are identical for uniaxial and equi-biaxial stress states but differ at other biaxial conditions as shown in Figure (1).

The limited data that has been generated has not provided any definite conclusion to the applicability of either theory, particularly at high temperature environment, where creep is encountered. Also, these theories do not account for the influence of anisotropy or for the rotation of principal axes in the case of non-synchronous loading systems.

Multiaxial data at room or high temperature is greatly influenced by test conditions and in the manner in which the test is conducted. Numerous methods have been suggested for multiaxial fatigue testing, but a very limited number have been carried out successfully.

METHOD OF MULTIAXIAL FATIGUE TESTING

The complexity of multiaxial fatigue testing led researchers to simplify the test requirements due to the fact that fatigue failure is generally originated at a point on the surface of a structure. For example, in the case of pressure vessels the state of stress is considered to be biaxial and since the surface of the structure is free from discontinuities or surface tractions, several types of tests were devised to produce this biaxial state of stress. Among the favorites are:

a - cylindrical specimens subjected to internal pressure, open-and closed-end cylinders

b - rotating disks

c - plate-type specimens such as bulging plate, wide cantilever plate, cruciform plate and rhombic plate

d - torsional tests of cylindrical specimens

CYLINDRICAL-TYPE SPECIMENS

In the case of testing cylindrical-type specimens under internal pressure, the state of biaxial stress is 2:1. This biaxial stress ratio falls in the first quadrant of the yield envelope and it is possible to alter this ratio by introducing a bending or axial stress. To develop a state of stress in the 2nd and 4th quadrant of the yield envelope, compressive external load or torsional loads have to be added to produce a negative stress. It has been shown that the addition of such loads could easily produce a buckling situation or a stress gradient that cannot be controlled. Investigators such as Morrison, Crossland, and Parry (2) used only pressurized tubes and they controlled the biaxiality ratio by the radius to thickness ratio. Their data is not comparable nor consistent with present controlled fatigue testing techniques. Their objective was to relate the endurance limit of the material to the biaxial state of stress. Esztergar (3) indicated in his literature survey on fatigue under biaxial stress cycling that the data produced was qualitative since crack initiation could not be detected and the large amount of autofrettage affected the crack propagation through the wall thickness; thus, the data was greatly influenced by these two obstacles. In the case of a part-through crack presence, the circumferential stress is increased locally, which results in a reduced hoop restraint that causes a tendency for bulging.

McKenzie et. al. (4) compared uniaxial and biaxial (shear) data from tests on thin-walled cylinders. They correlated their results on the basis of hysteresis loop energy per cycle. A distinct difference in fatigue life becomes apparent if the comparison is based on the octahedral plastic shear strain as shown in Figure (2).

Biaxiality ratio can also be altered if torsional loading is added; however, a new problem arises in the generated data. Axial strain is accumulated in reversed torsion. Specimens develop axial compressive stresses which result in higher cycle life. This effect was shown independently by Yokobori et. al. (5) and by Zamrik (6) using torsional test data of Halford and Morrow. Additional data for cylindrical specimen tests can be obtained from references (7).

FLAT-PLATE SPECIMENS

There are three types of tests that can be conducted utilizing the flat plate specimens, namely:

(1) the cantilever plate

(2) the Rhombic plate

(3) the circular or elliptical plate (oval plates)

In the first type, the biaxial stress ratio was produced by considering the ratio of transverse stress σ_T to longitudinal stress σ_L. By successfully decreasing the width w, the biaxiality ratio decreases. This approach was taken by Weiss et. al. (8) and their results are shown in Figures (3) and (4). Figure (4) shows a comparison between push-pull type uniaxial tests and plate bending tests. They also demonstrated that the decrease in fatigue endurance is associated with the increase in biaxiality ratios. This decrease can be correlated with the proportional loss in the static fracture ductility, ε_f, as shown in Figure (5).

Wide-beam-type specimens of pressure vessel steel materials were tested at Lehigh University (9). The stress ratios of 1:1 results are shown in Figure (6) on the basis of effective Von-Mises strain. They showed a slight reduction in the fatigue endurance of the lower-strength alloy and perhaps a greater effect on the high strength alloy (T-1). The data was reported on the basis of crack initiation.

Another type of plate specimen was developed by Zamrik et. al (10). The plate specimen known as the "rhombic" specimen showed a stress state in the second and fourth quadrants of the yield envelopes. The state of stress was produced by anticlastic bending as shown in Figure (7). Test data of three stress ratios from 0.1 to 1.0 were plotted on the basis of octahedral shear strain range and maximum strain range. The octahedral shear strain range shown in Figure (8) fitted the data well for all stress ratios. In the case of torsional data, the stress ratios exhibited a higher fatigue strength when compared to uniaxial fatigue data. The reason for this observation can be attributed to the degree of axial restraint imposed on the torsion specimen.

The rhombic plastic specimen is very attractive for biaxial testing since it affords simplicity in the loading system and provides a wide range of biaxial stress ratios.

Another type of plate specimen tested by Zamrik et. al (11) is the circular and elliptical specimen. For this type, shown in Figure (9a), pressure was applied to the specimen but the results showed a dependence on two variables: isotropy and Poisson's ratio as shown in Figure (9b). The method of analysis used in interpreting the flat plate specimen is described in appendix (A).

OUT-OF-PHASE STRAIN EFFECT

In some cases, particularly in temperature environment, the biaxial strain may become out-of-phase, e.g., non-synchronous loading as shown in

Figure (10); therefore, by applying the correlation used in analyzing the room temperature data, a large error may be produced in predicting the life of the material. A significant cause, in this case, is the distribution of the principal strain magnitudes and their directions, whereby a rotation of the principal strain axes takes place. The surface element of the material takes a new orientation and the maximum and minimum principal strains occur at different times as shown in Figure (11). The limited data available for phase angles of 0 to 90° was analyzed by Zamrik (12) on the basis of maximum total strain:

$$\varepsilon_T = \sqrt{[\varepsilon_1^2 + \varepsilon_2^2 + \varepsilon_3^2]}$$

A correlation, similar to that of Manson-Coffin relation, was obtained with the constants ($a \cong 0.3$, $c = \varepsilon_f \sqrt{1.5}$) as shown in Figure (12). The reasonable fit of the data for the entire range indicates that the damage mechanism in multiaxial fatigue may be similar to the uniaxial case even though the stress (strain) axis was rotated. This interpretation may be considered conclusive if and only when actual non-synchronous data at high temperature becomes available.

ENGINEERING CORRELATIONS

a - <u>Maximum Shear Stress Theory</u> (Tresca)

The theory predicts yield condition when the shear stress on any plane reaches the uniaxial yield stress. Therefore, the following condition exists for maximum and minimum principal stresses:

$$\tau = \frac{1}{2}(\sigma_1 - \sigma_3) = \frac{1}{2}\sigma_y$$

The equivalent stress and strain are defined as:

$$\bar{\sigma} = \sigma_1 - \sigma_3 = 2\tau$$

$$\bar{\varepsilon} = k\ (\varepsilon_1 - \varepsilon_3)$$

b - <u>Distortion Energy Theory</u> (Von-Mises)

$$\gamma_o = \frac{2}{3}\ [(\varepsilon_1 - \varepsilon_2)^2 + (\varepsilon_2 - \varepsilon_3)^2 + (\varepsilon_3 - \varepsilon_1)^2]^{\frac{1}{2}}$$

For low cycle fatigue condition, one assumes a constant volume and Poisson's ratio of $1/_2$:

$$\varepsilon_1 + \varepsilon_2 + \varepsilon_3 = 0$$

For a biaxial case, a strain range ratio can be introduced in the form of:

$$\phi = \frac{\Delta\varepsilon_2}{\Delta\varepsilon_1}$$

and $\Delta\gamma_o = \frac{2\sqrt{6}}{3}\ (\phi^2 + \phi + 1)^{\frac{1}{2}}\ \Delta\varepsilon_1$

The effective strain range, $\Delta\varepsilon_e$, which is another form of the octahedral shear strain range, has a form:

$$\Delta\bar{\varepsilon}_e = \frac{2}{\sqrt{3}}\ (\phi^2 + \phi + 1)^{\frac{1}{2}}\ \Delta\varepsilon_1$$

or $$\Delta\bar{\varepsilon}_e = \frac{1}{\sqrt{2}}\ \Delta\gamma_o$$

on the basis of tests shown in Figure (8), a relation between unaxial and biaxial data can be derived in the following procedure:

$$(\Delta\gamma_o)_{uni} = \sqrt{2}\ \Delta\varepsilon$$

utilizing Manson's relation:

$$\Delta\epsilon N^{z} = C_1$$

then $$(\Delta\gamma_o)_{uni} = \frac{\sqrt{2}\,C_1}{N^{z}} = \frac{C}{N^{z}}$$

where $$C = \sqrt{2}\,C_1$$

if failure under multiaxial strain cycling can be defined to occur when:

$$(\Delta\gamma_o)_{multi} = (\Delta\gamma_o)_{uni}$$

then multiaxial strain cycling can be related to the number of cycles to failure N_f in a relation such as:

$$(\Delta\gamma_o)_{multi}\ N_f^{\,z} = C$$

CONCLUDING REMARKS

Multiaxial fatigue testing is a complex technique where the utmost care must be considered in analyzing the data. Variables such as anisotropy, Poisson's ratio, strain accumulation, crack initiation in cylindrical specimens, ..., must be monitored and accounted for. These variables have minimum influence on uniaxial fatigue data.

The static yield theories should be used conservatively since they are not designed for fatigue analysis, particularly in the presence of high temperature environment.

REFERENCES

1. S. S. Manson, "Behavior of Materials Under Conditions of Thermal Stress," NASA Technical Note 2933, 1954.

2. J. L. M. Morrison, B. Crossland, and J. S. Parry, "Strength of Thick Cylinders Subjected to Repeated Internal Pressures," J. Eng. Ind. 82, 143-53 (1960).

3. E. P. Esztergar, "Creep-Fatigue Interaction and Cumulative Damage Evaluations for Type 304 Stainless Steel," ORNL-4757, (1972).

4. C. T. MacKenzie, D. J. Burns, and P. P. Benham, "A Comparison of Uniaxial and Biaxial Low-Endurance Fatigue Behavior of Two Steels," Proc. Inst. Mech. Eng. 180, 414-23 (1966).

5. T. Yokobori, H. Yamanovchi, and S. Yamamoto, "Low-Cycle Fatigue of Thin-Walled Cylindrical Specimens of Mild Steel," Int. J. Fract. Mech. 1, 3-13 (1965).

6. S. Y. Zamrik and T. Goto, "The Use of Octahedral Shear Strain Theory in Biaxial Low Cycle Fatigue," pp. 551-62, Proc. of Inter-American Conference on Materials Technology," ASME 1968.

7. K. J. Pascoe and J. W. R. de Villiers, "Low-Cycle Fatigue Testing of Steel Under Biaxial Straining," J. Strain Anal. 2, 117-26 (1967). M. B. Reynolds, "Strain-Cycle Phenomena in Thin-Walled Tubing," GEAP-4462 (1964).

8. V. Weiss, J. Sessier, and P. Packman, "Low Cycle Fatigue of Pressure Vessels Material," TID-16455 (1962).

9. K. D. Ives and J. T. Tucker, "Equibiaxial Low-Cycle Fatigue Properties of Typical Pressure-Vessel Steels," ASME 65-MET-19, (1965).

10. S. Y. Zamrik, "Advances in Design For Elevated Temperature Environment," ASME, Sep. Publ. June 23-27, (1975).

11. J. Shewchuck, S. Zamrik, and J. Marin, "Low Cycle Fatigue of 7075-T651 Aluminum Alloy in Biaxial Bending," Exp. Mech. 8 504-12 (1968).

12. S. Y. Zamrik, and R. E. Frishmuth, "The Effects of Out-of-Phase Biaxial Strain Cycling on Low Cycle Fatigue," Exp. Mech. 13 (5): 204-208, (1973).

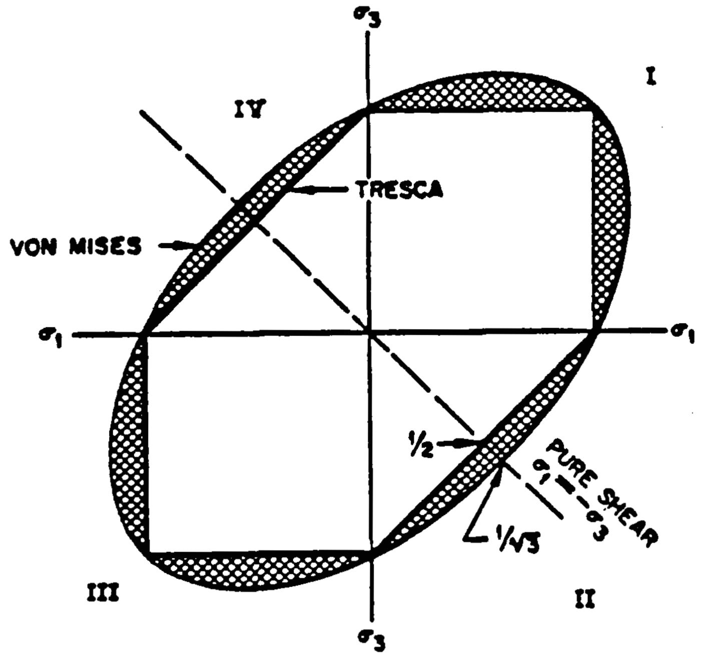

Fig. 1. Tresca and von Mises yield criteria.

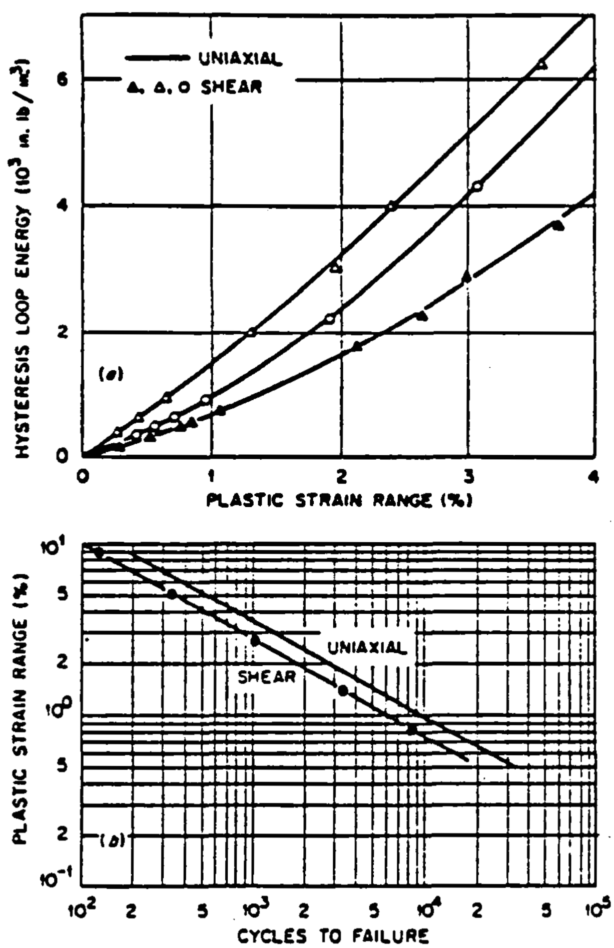

Fig. 2. Comparison of uniaxial and biaxial fatigue life of 2 1/2 Ni—Cr—Mo (Ref. 4).

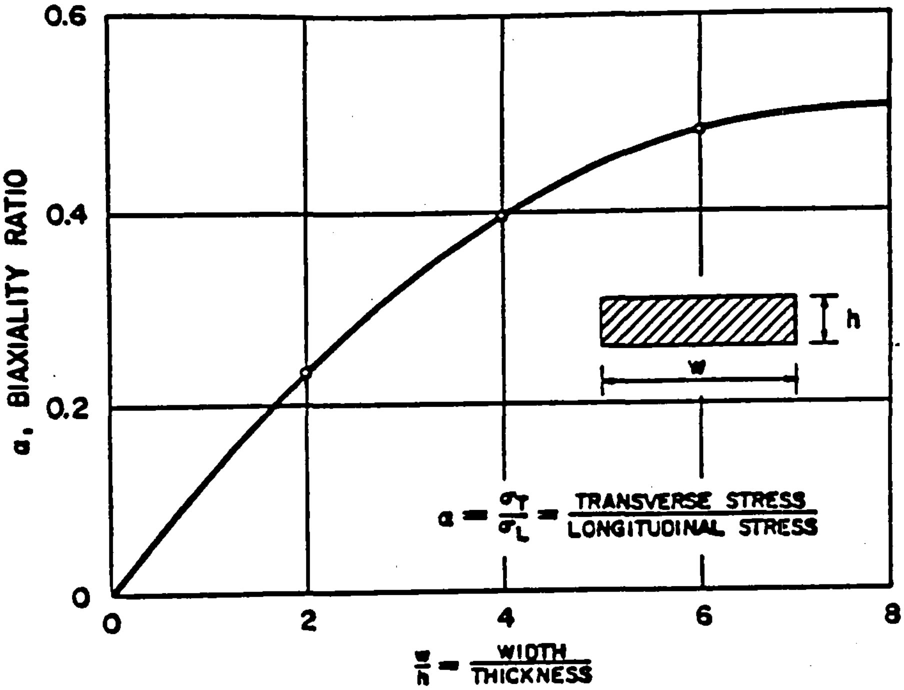

Fig. 3. Biaxiality of a bend plate (Ref. 8).

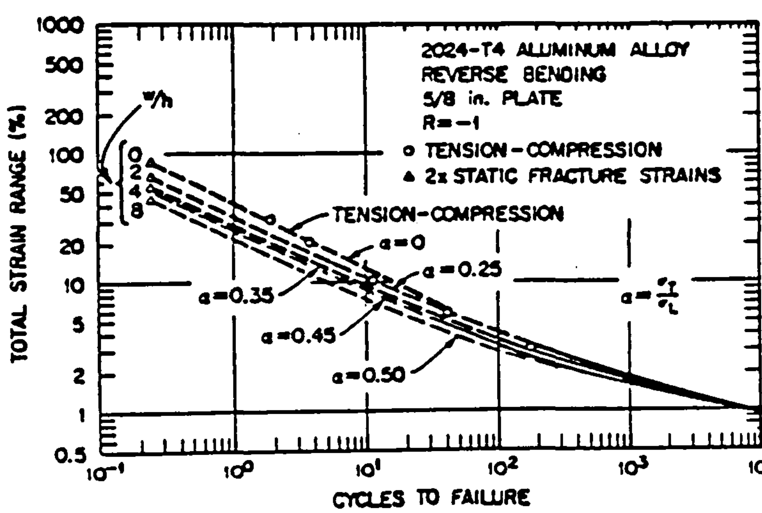

Fig. 4. Biaxial fatigue strength of aluminum (Ref. 8).

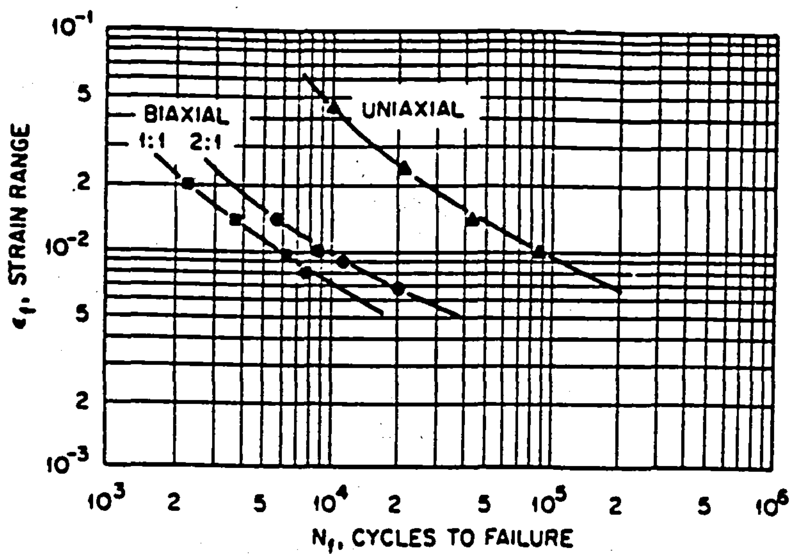

Fig. 5. Biaxial fatigue endurance of 301 stainless steel (Ref. 3).

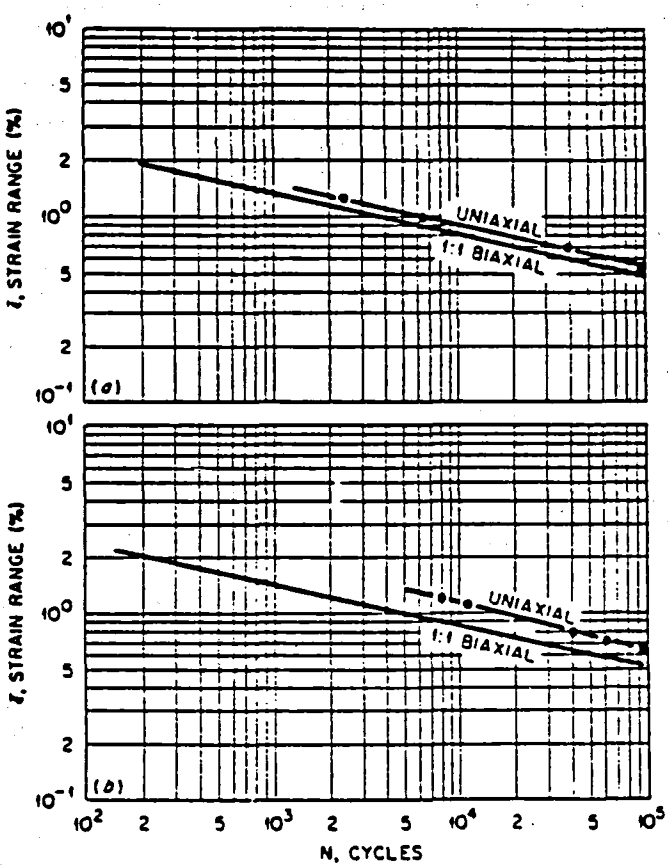

Fig. 6. Biaxial fatigue life of (a) A-302 carbon steel and (b) T-1 alloy (Ref. 9).

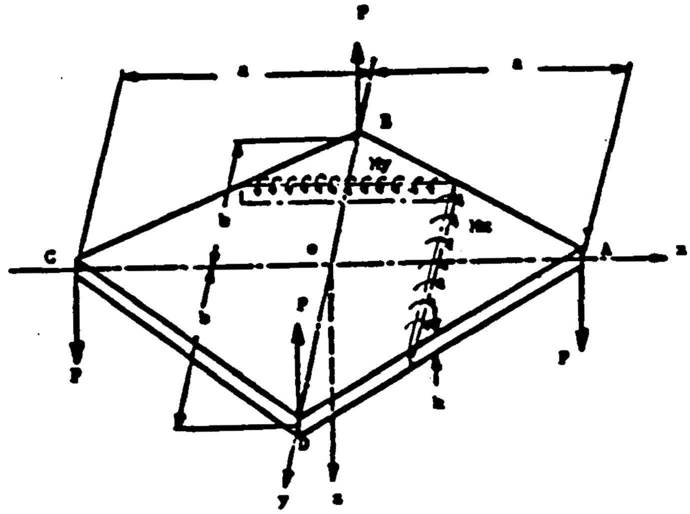

Fig. 7. A rhombic plate subjected to anticlastic bending

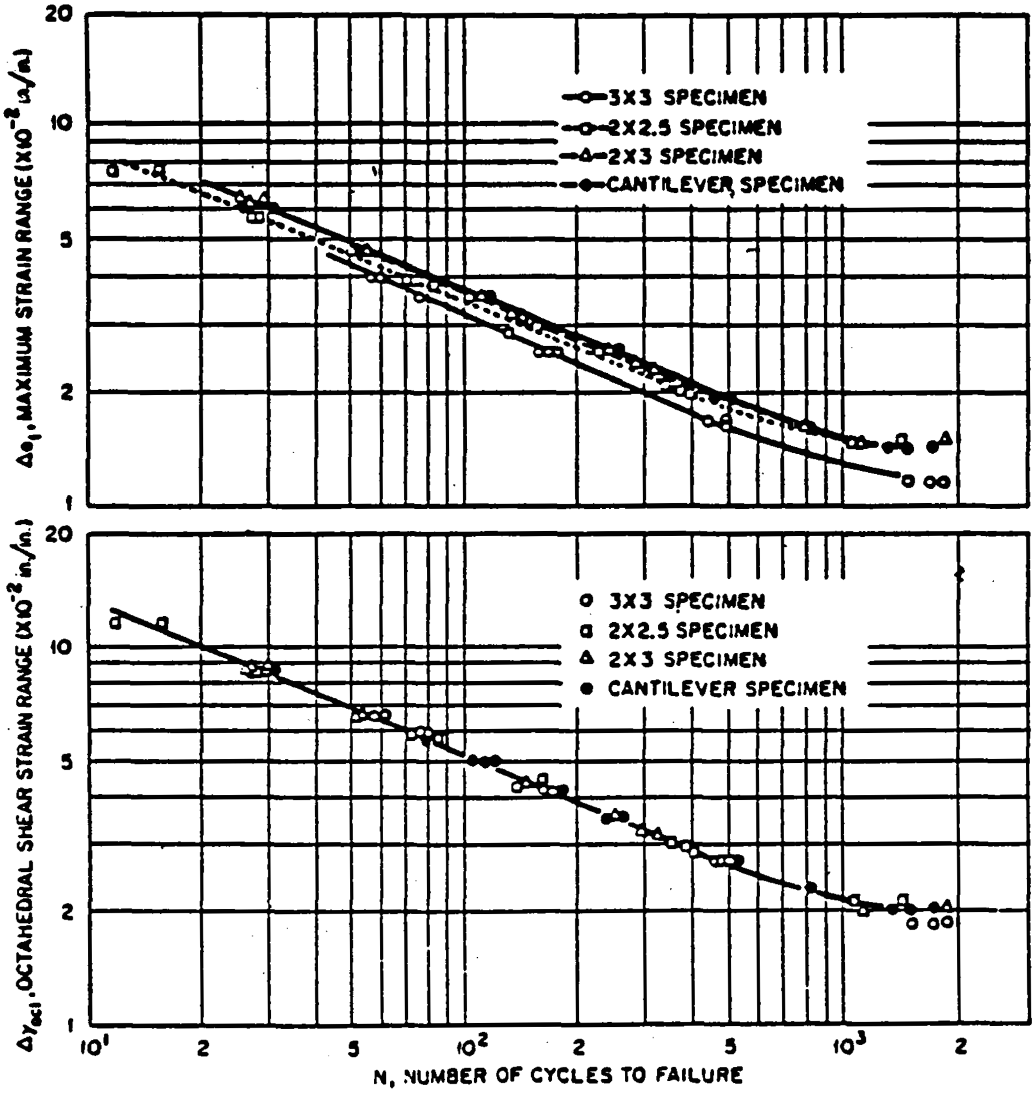

Fig. 8. Comparison of low-cycle fatigue data based on (a) maximum strain range and (b) octahedral shear strain range (Ref. 6).

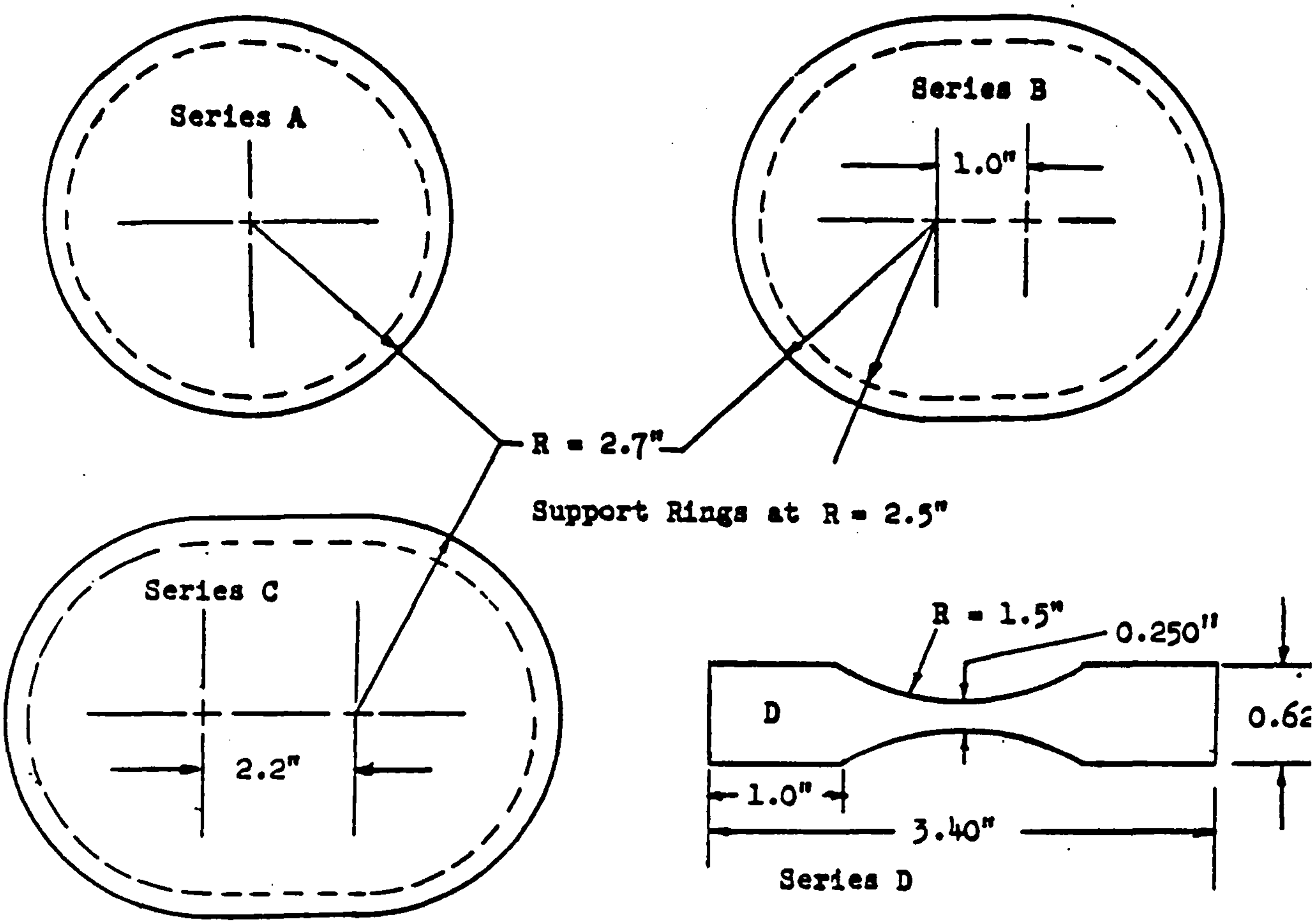

Figure 9a. Circular & Elliptical plate specimens.

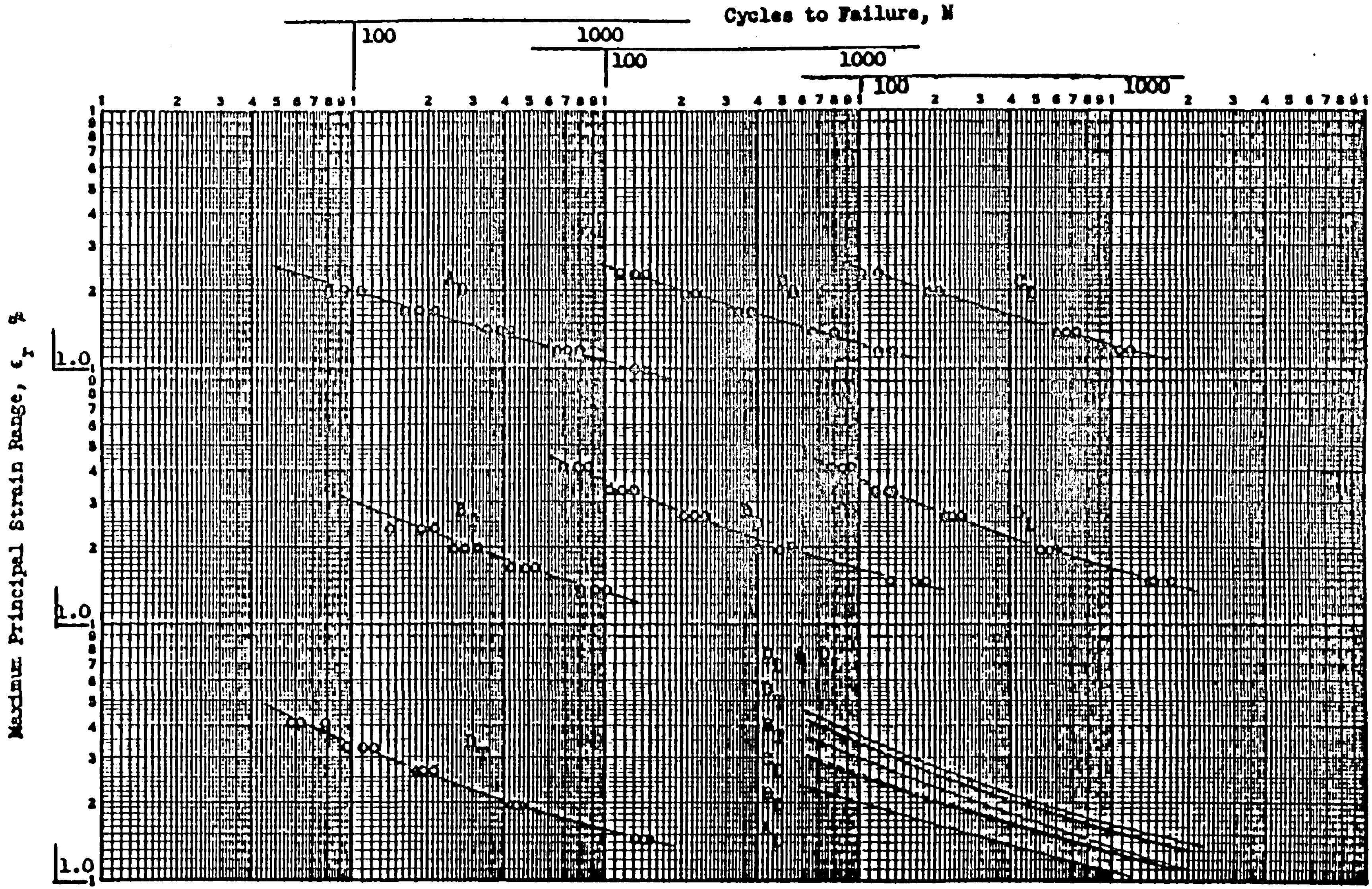

Figure 9b. Maximum Principal Strain Range vs. Cycles to Failure for 7075-T651 Aluminum Alloy in Bending (11).

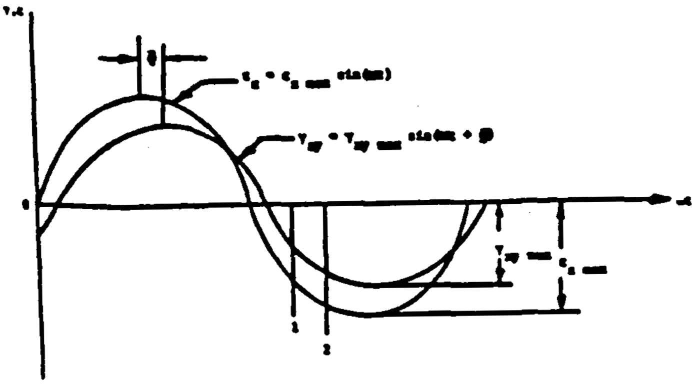

Fig. 10 Out-of-phase straining condition

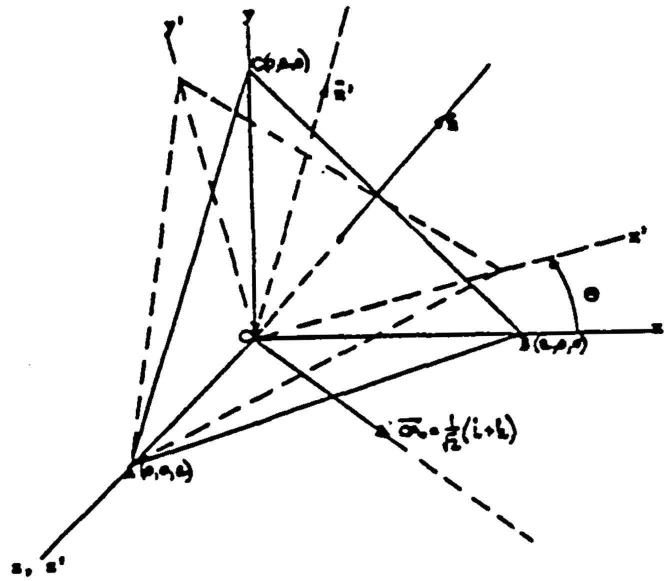

Fig. 11 Rotation of principal axes due to out-of-phase straining condition

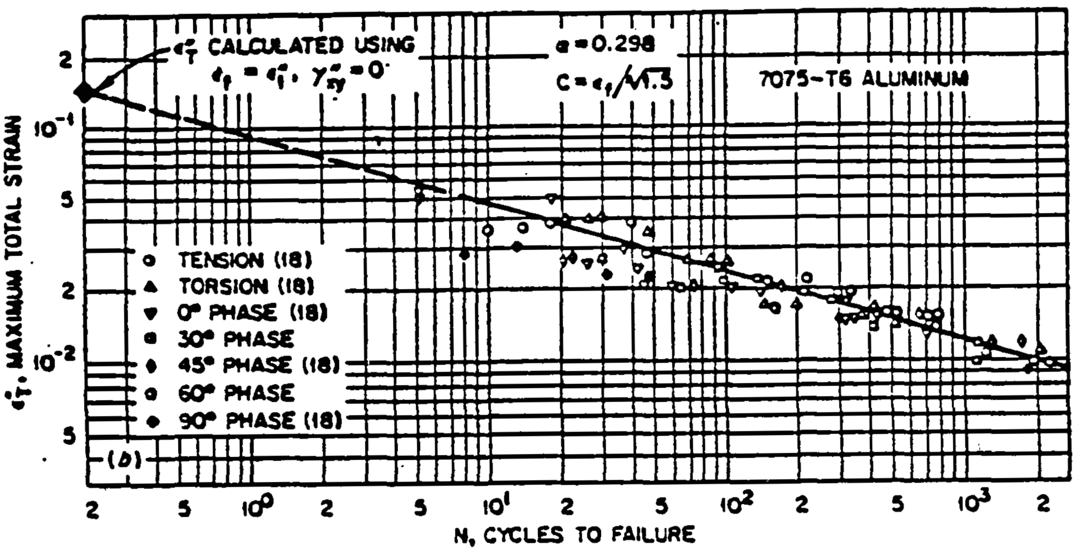

Fig. 12. Maximum total strain vs cycles to failure using experimental data from various phase angle tests. Both coordinates are logarithmic (Ref. 12).